Available online at www.sciencedirect.com
ScienceDirect
Journal of Sound and Vibration 309 (2008) 887–895
JOURNAL OF SOUND AND VIBRATION
www.elsevier.com/locate/jsvi

Short Communication

On the response and dissipated energy of Bouc–Wen hysteretic model

A.E. Charalampakis, V.K. Koumousis*

National Technical University of Athens, Athens, Greece

Received 9 May 2007; received in revised form 23 July 2007; accepted 31 July 2007

Abstract

An efficient formulation for the response and dissipated energy of Bouc–Wen hysteretic model is proposed. The displacement is associated with the hysteretic parameter in terms of Gauss' hypergeometric function. The hysteretic equation is solved analytically for specific values of the exponential parameter that controls the transition between elastic and inelastic regime. This formulation is used to provide analytical expressions of the dissipated energy under symmetric cyclic excitation, based solely on the model parameters and the displacement amplitude. For arbitrary values of the exponential parameter, the equations are solved numerically. For fully yielding systems, approximate relations are determined using suitable curve fitting. The derived expressions facilitate considerably the preliminary design of hysteretic systems.

1. Introduction

The Bouc–Wen model is a smooth endochronic model that is often used to describe hysteretic phenomena. It was introduced by Bouc [1] and extended by Wen [2], who demonstrated its versatility by producing a variety of hysteretic patterns. The model has been successfully employed in many areas of engineering, as for example in reinforced concrete and steel structures [3,4], base isolation systems [5], wood joints [6], magnetorheological fluid dampers [7], etc. The hysteretic behavior is treated in an unified manner by a single nonlinear differential equation with no need to distinguish different phases, as for example in the various Coulomb friction models [8].

In this study, the displacement of the system is expressed as a hypergeometric function of the hysteretic parameter. Analytical solutions are provided for specific values of the exponential parameter. For arbitrary values of the latter, efficient techniques are employed for the numerical solution of the derived equation. Thus, the hysteretic response can be evaluated accurately for large displacement steps rather than infinitesimal ones. Using this formulation, the dissipated energy under symmetric cyclic excitation can be determined analytically. This allows for the accurate evaluation of the dissipated energy of hysteretic systems. Finally,

*Corresponding author. Tel.: +30 2107721657; fax: +30 2107721651.
E-mail address: vkoum@central.ntua.gr (V.K. Koumousis).

0022-460X/$ - see front matter
doi:10.1016/j.jsv.2007.07.080

a parametric study that associates the dissipated energy with the displacement amplitude is conducted and the results are discussed.

2. Model formulation

The restoring force $F(t)$ of a single-degree-of-freedom system can be expressed as

$$F(t) = a\frac{F_y}{u_y}u(t) + (1-a)F_y z(t), \tag{1}$$

where $u(t)$ is the displacement, F_y the yield force, u_y the yield displacement, a the ratio of post-yield to pre-yield (elastic) stiffness and $z(t)$ a dimensionless hysteretic parameter that obeys a single nonlinear differential equation:

$$\dot{z}(t) = \frac{1}{u_y}[A - |z(t)|^n(\beta + \text{sign}(\dot{u}(t)z(t))\gamma)]\dot{u}(t), \tag{2}$$

where A, β, γ, n are dimensionless quantities controlling the behavior of the model, sign($\cdot$) is the signum function and the overdot denotes the derivative with respect to time. Small values of the positive exponential parameter n correspond to smooth transition from elastic to post-elastic branch, whereas for large values of n the transition becomes abrupt, approaching that of the bilinear model. Parameters β, γ control the size and shape of the hysteretic loop. Parameter A was introduced in the original paper, but it became evident that it is redundant [9].

It follows from Eq. (1) that the restoring force $F(t)$ can be analyzed into an elastic and a hysteretic part as follows:

$$F^{el}(t) = a\frac{F_y}{u_y}u(t), \tag{3}$$

$$F^h(t) = (1-a)F_y z(t). \tag{4}$$

Thus, the model can be visualized as two springs connected in parallel (Fig. 1), where $k_i = F_y/u_y$ and $k_f = ak_i$ are the initial and post-yielding stiffness of the system.

3. Parameter constraints

It has been shown in formal mathematical manner that the parameters of Bouc–Wen model are functionally redundant; there exists a multiplicity of parameter vectors that produce an identical response for a given

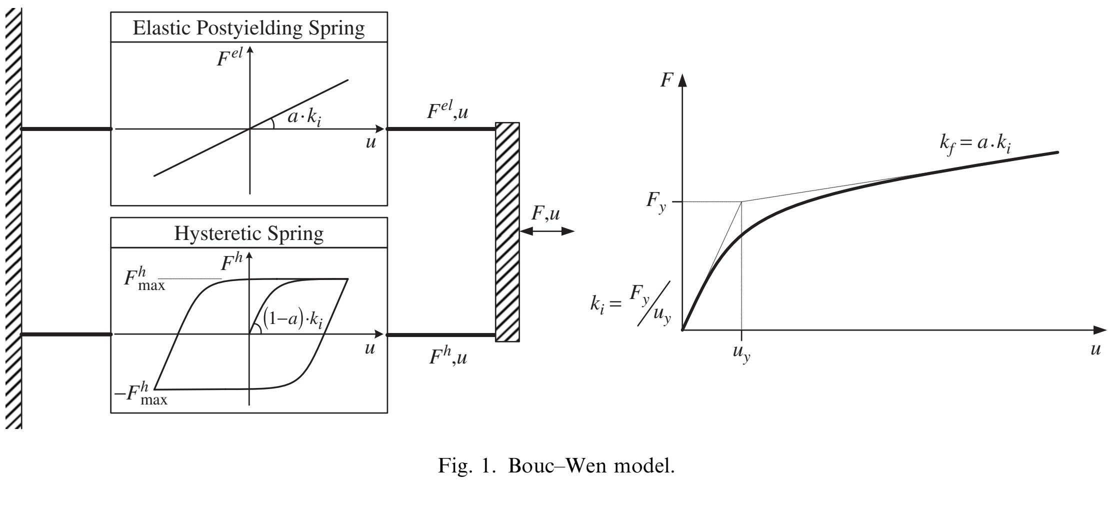

Fig. 1. Bouc–Wen model.

excitation [9]. Removing this redundancy is best achieved by fixing parameter A to unity [9]. Henceforth, this constraint is assumed to hold.

Further, by modifying parameters β and γ one can produce hysteretic loops with strain-hardening, as demonstrated by Wen [2]. However, these parameters do not have clear physical interpretation. Early studies by Constantinou and Adnane [10] suggested imposing a certain constraint, viz., $A/(\beta+\gamma)=1$, to reduce the model to a formulation with well-defined properties. This constraint is also adopted herein. Strain hardening can be achieved by more efficient techniques, such as the introduction of a dedicated spring; an example of this approach can be found in Sivaselvan and Reinhorn [11].

Thus, the extrema of the hysteretic parameter are obtained by setting $\dot{z}=0$ in Eq. (2) as follows:

$$z_{\text{ext}} = \pm\left(\frac{A}{\beta+\gamma}\right)^{1/n} = \pm 1. \tag{5}$$

Although not strictly adopted in this study, thermodynamic admissibility issues impose the following inequality [12]:

$$\gamma \geqslant \beta. \tag{6}$$

Based on Eq. (6), the hysteretic loop assumes a bulge shape as opposed to a slim-S one.

4. Response

At any time instant, the behavior of Bouc–Wen model can be partitioned into four segments depending on the sign of $\dot{u}$ and z. In illustration, the response under cyclic excitation is shown in Fig. 2, where the dotted line signifies the path of the elastic response. Points A and C signify sign reversal of velocity $\dot{u}$ whereas points B and D signify sign reversal of hysteretic force F^h or, equivalently of hysteretic parameter $z\in[-1,1]$. Since the calculation of the elastic response is trivial, the analysis presented herein focuses in the response of the hysteretic spring only.

In the non-trivial case of $\beta\neq\gamma$ and by omitting time, Eq. (2) can be expressed as

$$\mathrm{d}u = \frac{u_y}{1-|z|^n(\beta+\text{sign}(\dot{u}z)\gamma)}\,\mathrm{d}z. \tag{7}$$

The indefinite integral of Eq. (7) can be expressed analytically in terms of Gauss' hypergeometric function ${}_2F_1(a,b,c;w)$. Accounting for initial conditions, Eq. (7) can be written in the form:

$$\frac{u-u_0}{u_y} = z\,{}_2F_1\left(1,\frac{1}{n},1+\frac{1}{n};q|z|^n\right)\Bigg|_{z_0}^{z}, \tag{8}$$

where $q=\beta+\text{sign}(\dot{u}z)\gamma$ and u_0, z_0 are the initial values of the displacement and hysteretic parameter, respectively. Eq. (8) is solved analytically for z for specific values of the exponential parameter n. For $n=1$, one obtains:

$$z = \frac{\text{sign}(z)+(qz_0-\text{sign}(z))\,\mathrm{e}^{-(\text{sign}(z)q(u-u_0)/u_y)}}{q}. \tag{9}$$

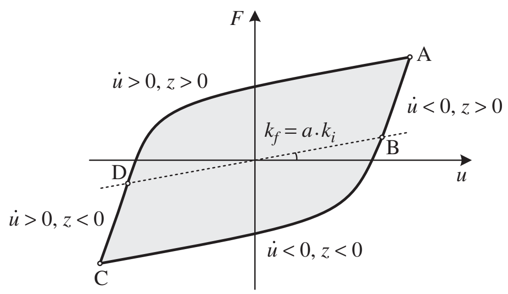

Fig. 2. Response of Bouc–Wen model under cyclic excitation.

Table 1
Signum values and domain of z per segment

Segment	q	sign(z)	Domain
AB	$\beta-\gamma$	1	$z_0 \in [0,1], z \in [0, z_0]$
BC	1	-1	$z_0 \in (-1,0], z \in (-1, z_0]$
CD	$\beta-\gamma$	-1	$z_0 \in [-1,0], z \in [z_0, 0]$
DA	1	1	$z_0 \in [0,1), z \in [z_0, 1)$

For $n=2$, z is given by

$$z = \frac{\tanh\left(\sqrt{q}(u-u_0)/u_y + \operatorname{arctanh}\left(\sqrt{q}z_0\right)\right)}{\sqrt{q}}, \tag{10}$$

where tanh(·), arctanh(·) are the normal and inverse hyperbolic tangent, respectively. In Eq. (10), $\sqrt{q}$ may be complex but the result is real. Special attention must be paid with respect to the values of signum and the domain of hysteretic parameter z per segment (Table 1).

For arbitrary values of n, Eq. (8) must be solved numerically. An inspection of Eq. (2) shows that, given $\gamma \in (0,1]$, the hysteretic parameter z is a continuous and strictly monotonic function of displacement u. Thus, there exists a single root, if any, of Eq. (8) within the domain of z and the latter can be evaluated efficiently by bisection-type methods. The Van Wijngaarden–Dekker–Brent method [13], which combines bisection and inverse quadratic interpolation, typically requires few steps to yield z in double precision accuracy.

It is important to note that, considering the hypergeometric function ${}_2F_1(a,b,c;w)$, point $w(1,0)$ is singular in the complex plane and the limit needs to be evaluated as $w \to 1^-$ [14]. Proper evaluation techniques are provided in Appendix A. In particular, when loading in either direction, root bracketing is attempted with extremum value of z equal to $\pm(1-\varepsilon)$, where ε is machine epsilon. If this fails, then the system has yielded fully and $z = \pm 1$ is assumed. When unloading, if root bracketing fails, then there is a segment transition, i.e. from AB to BC, or from CD to DA, and z needs to be evaluated in two steps.

In the special case of $\beta = \gamma = 1/2$, the unloading branches are straight lines and integration of Eq. (7) yields:

$$z = \frac{(u-u_0)}{u_y} + z_0. \tag{11}$$

Eq. (11) is independent of n. The loading branches are covered by Eq. (8).

5. Dissipated energy

The dissipated energy is expressed by the area enclosed by hysteretic loops. Generic analytical expressions of the dissipated energy will be derived with respect to the steady-state response under symmetric wave T-periodic input [15]. This class of inputs is common in identification procedures and includes sine waves, triangular inputs, etc. Under a T-periodic excitation the response is asymptotically T-periodic and the hysteretic loop is traced repeatedly [15].

The post-yielding spring of Fig. 1 does not dissipate energy and can be ignored. Thus, only the response of the hysteretic spring is considered (Fig. 3), where the displacement amplitude $u_{\max}$ is common in both directions and $F^h_{\max} = (1-a)F_y$ is the maximum hysteretic force. As in the preceding section, points A and C signify sign reversal of velocity $\dot{u}$, whereas points B and D signify sign reversal of hysteretic parameter $z \in [-1,1]$. The maximum value of the latter, occurring at point A, corresponds to the maximum displacement. Making use of symmetry, it follows that $u_A = -u_C = u_{\max}$ and $z_A = -z_C$, where the subscript denotes the corresponding point of the hysteretic loop. Considering the transition from point C to point A and employing Eq. (8), one obtains:

$$\frac{u_{\max}}{u_y} = \frac{z_A}{2}\left({}_2F_1\left(1, \frac{1}{n}, 1+\frac{1}{n}; (\beta-\gamma)z_A^n\right) + {}_2F_1\left(1, \frac{1}{n}, 1+\frac{1}{n}; z_A^n\right)\right), \tag{12}$$

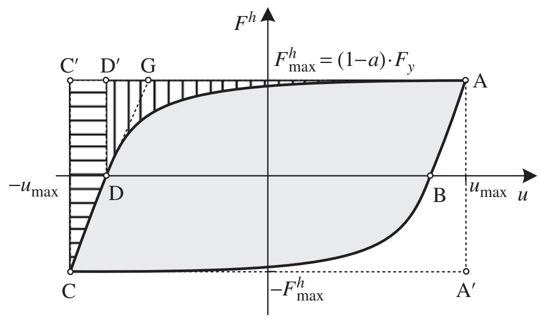

Fig. 3. Steady-state response of hysteretic spring under symmetric wave T-periodic excitation.

where z_A is the unknown maximum value of hysteretic parameter z. There exist several analytical expressions of z_A for specific values of n and $(\beta-\gamma)$. In general, however, numerical evaluation must be employed. In similar manner, as in the preceding section, the Van Wijngaarden–Dekker–Brent method [13] is employed which converges rapidly. If root bracketing with $z_A \in [0, 1-\varepsilon]$ fails, then full yield is assumed and z_A is taken equal to unity.

Further, the dissipated energy during a complete cycle can be expressed in terms of z_A. The enclosed area is given by

$$E = \oint F^h \, \mathrm{d}u. \tag{13}$$

Attempting to change variable and integrate in terms of z leads to a formulation that is inappropriate for fully yielding systems. This is because, for large values of the displacement, z_A is very close to unity and thus difficult to evaluate numerically with sufficient accuracy. An alternative method that eliminates this problem is to evaluate the complementary areas, i.e. the dashed areas of Fig. 3, and subtract them from the outer rectangle. Making use of symmetry, the dissipated energy is then expressed as follows:

$$E = 4F^h_{\max}u_{\max} - 2\int_{u_C}^{u_A} (F^h_{\max} - F^h)\, \mathrm{d}u. \tag{14}$$

Restricting attention to segment CD, the complementary area is given by

$$E_{\overparen{D'C'CD}} = F^h_{\max}u_y \int_{-z_A}^{0} \frac{(1-z)}{1-(-z)^n(\beta-\gamma)}\, \mathrm{d}z. \tag{15}$$

The integral of Eq. (15) can be expressed in terms of Gauss' hypergeometric function ${}_2F_1(a,b,c;w)$ as follows:

$$E_{\overparen{D'C'CD}} = F^h_{\max}u_y k^*_{CD}, \tag{16}$$

where

$$k^*_{CD} = z_A\, {}_2F_1\left(1, \frac{1}{n}, 1+\frac{1}{n}; (\beta-\gamma)z_A^n\right) + \frac{1}{2}z_A^2\, {}_2F_1\left(1, \frac{2}{n}, 1+\frac{2}{n}; (\beta-\gamma)z_A^n\right), \tag{17}$$

When the system yields fully, it follows that $z_A \cong 1$ and parameter k^*_{CD} is a function of n and γ only (Fig. 4a). Further, when $\beta = \gamma = 1/2$ the unloading branch is a straight line with stiffness equal to $F^h_{\max}/u_y$. In this case, Eq. (16) yields $3/2F^h_{\max}u_y$ (independent of n), i.e. the area of trapezoid $D'C'CD$ (Fig. 3).

Following similar formulation for segment DA, the complementary area is evaluated as

$$E_{\overparen{AD'D}} = F^h_{\max}u_y \int_0^{z_A} \frac{(1-z)}{1-z^n}\, \mathrm{d}z. \tag{18}$$

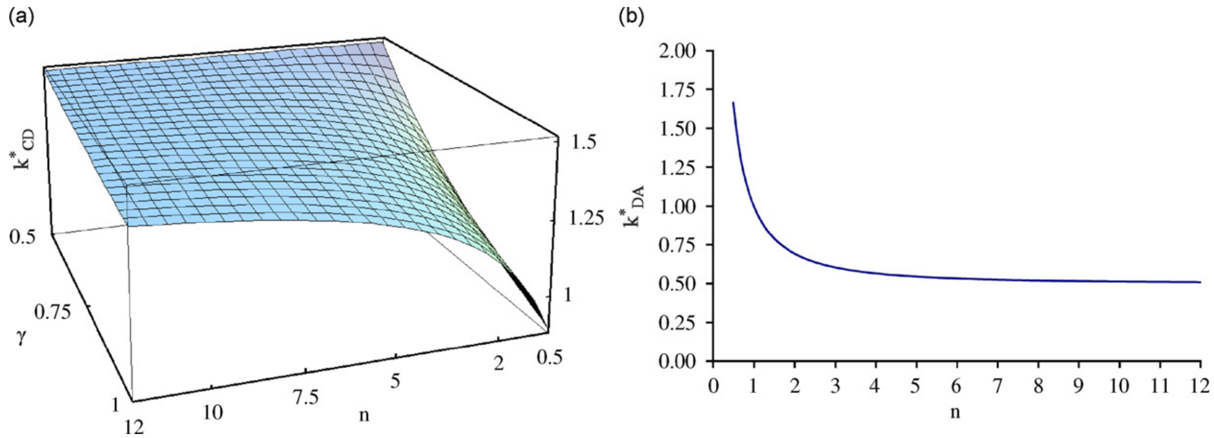

Fig. 4. (a) Parameter k^*_{CD} as a function of n, γ (b) Parameter k^*_{DA} as a function of n (full yield).

Table 2
Parameter k^*_{DA} for various values of n (full yield)

n	k^*_{DA} (analytical)	k^*_{DA} (numerical)
$\frac{1}{2}$	$\frac{5}{3}$	1.666667
1	1	1.000000
$\frac{3}{2}$	$2(1-\sqrt{3}\pi/9)$	0.790800
2	$\ln(2)$	0.693147
3	$\sqrt{3}\pi/9$	0.604600
4	$(\pi+\ln(4))/8$	0.565986
6	$(\sqrt{3}\pi+\ln(64))/18$	0.533349
12	$(2\pi+\ln(4)-\sqrt{3}\ln(7-4\sqrt{3}))/24$	0.509648

Eq. (18) takes the form:

$$E_{\widehat{AD'D}} = F^h_{\max} u_y k^*_{DA}, \tag{19}$$

where

$$k^*_{DA} = z_A\, {}_2F_1\left(1, \frac{1}{n}, 1+\frac{1}{n}; z_A^n\right) - \frac{1}{2} z_A^2\, {}_2F_1\left(1, \frac{2}{n}, 1+\frac{2}{n}; z_A^n\right). \tag{20}$$

It should be emphasized that, when the system yields fully and $z_A \to 1^-$, the limit of Eq. (20) is bounded and can be evaluated numerically (Fig. 4b). Closed-form solutions can also be derived for specific values of n (Table 2). Further, as n increases the transition between elastic and post-elastic branches becomes abrupt and it is observed that parameter k^*_{DA} approaches 1/2 asymptotically. At the limit, Eq. (19) yields $1/2F^h_{\max}u_y$, i.e. the area of triangle $GD'D$ (Fig. 3).

Thus, based on the derived complementary areas, Eq. (14) assumes the form:

$$E = 2F^h_{\max} u_y \left(2\frac{u_{\max}}{u_y} - k^*_{CD} - k^*_{DA}\right). \tag{21}$$

Eq. (21) can be employed for both partially and fully yielding systems. Particularly for the latter case, parameters k^*_{CD} and k^*_{DA} can be provided by simple approximate functions. These are derived using standard

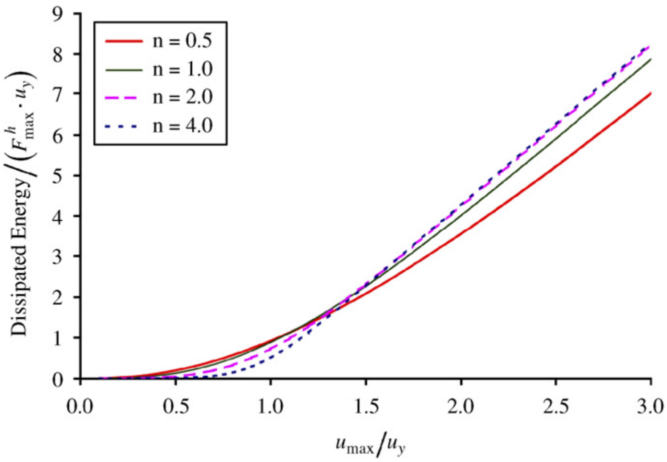

Fig. 5. Dissipated energy as a function of displacement amplitude ($\beta = 0.1$, $\gamma = 0.9$).

curve-fit techniques, as follows:

$$k^*_{CD} \cong \frac{0.003\ \ln(n) - 1.784\ \ln(\gamma) - 1.238}{1 + 0.89n + 0.592\gamma} + 1.5, \quad n \in [0.5, 12], \quad \gamma \in [0.5, 1.0], \tag{22}$$

$$k^*_{DA} \cong \frac{126.57 + 87.66n + 35.96n^2}{1.0 + 177.37n + 71.83n^2}, \quad n \in [0.5, 12], \tag{23}$$

where $\ln(\cdot)$ is the natural logarithm. The maximum relative error of Eq. (22) is less than 0.4%, while Eq. (23) is even more accurate, providing precision to the third decimal digit.

6. Results and discussion

Summarizing, the hysteretic response under imposed displacement can be determined using Eq. (8). This equation is solved analytically for $n = 1$ and 2. For arbitrary values of n, the equation can be solved numerically by employing efficient procedures.

Considering the steady-state response under symmetric cyclic excitation, the unknown maximum value of parameter z is determined from Eq. (12). The dissipated energy is then given by Eq. (21), i.e. by calculating the complementary areas and subtracting them from the outer rectangle. This formulation is numerically stable for both partially and fully yielding systems. For the latter case, which is usually encountered, parameters k^*_{CD} and k^*_{DA} can be derived with sufficient accuracy from Eqs. (22) and (23), respectively.

By employing the methods presented herein, the dissipated energy per cycle can be determined based solely on the displacement amplitude $u_{\max}$ and parameter vector $\mathbf{p} = \{\gamma, n, a, F_y, u_y\}$. Thus, the preliminary design of hysteretic systems is facilitated considerably, as for example in the case of base isolation systems of buildings or bridges. Typically, the super-structure is assumed rigid. Based on identified Bouc–Wen parameters, the proposed method yields more realistic results as compared to the simple bilinear model which is commonly used [16].

Further, the dissipated energy is presented in Fig. 5 as a function of the displacement amplitude for several values of the exponential parameter n. Both axes are normalized, while parameter γ is taken equal to 0.9 in all cases.

It is noted that, as the displacement amplitude increases, all curves become straight and parallel lines with a common slope equal to four. This is expected because, for a fully yielding system, an increase in displacement amplitude $\Delta u_{\max}$ would result in an increase $\Delta E = 4F^h_{\max}\,\Delta u_{\max}$ of the area enclosed by the hysteretic loop

(Fig. 3). Further, as parameter n increases, the response of the system approaches that of the bilinear model and thus the dissipated energy diminishes for $u_{\max}/u_y < 1$.

Acknowledgements

This work has been funded by the project PENED 2003. The project is co-financed by 75% of public expenditure through EC-European Social Fund, 25% of public expenditure through Ministry of Development-General Secretariat of Research and Technology and through private sector, under measure 8.3 of Operational Programme "Competitiveness" in the third Community Support Programme.

Appendix A. Evaluation of hypergeometric function

In this study, one is interested in the evaluation of ${}_2F_1(a,b,c;w)$ for real values of $w \in (-\infty, 1)$. The hypergeometric function is the analytical continuation of the so-called hypergeometric series [14]:

$$ {}_2F_1(a,b,c;w) = \sum_{n=0}^{\infty} \frac{(a)_n (b)_n}{(c)_n} \frac{w^n}{n!}, \tag{24}$$

where $(w)_n = w(w+1)(w+1)\ldots(w+n-1), (w)_0 = 1$ is Pochhammer's symbol and $n!$ the factorial of n. Although the circle of convergence of the above series is the unit circle $|w|$, its rate of convergence is satisfactory only for $|w| \leqslant 1/2$ [13]. For $w \in (1/2, 1)$, the values are produced by linear transformation. In the cases presented herein, $c = a + b$ and hence the following formula is used [14]:

$$ {}_2F_1(a,b,a+b;w) = \frac{\Gamma(a+b)}{\Gamma(a)\Gamma(b)} \sum_{n=0}^{\infty} \frac{(a)_n (b)_n}{(n!)^2} \times [2\psi(n+1) - \psi(a+n) - \psi(b+n) - \ln(1-w)](1-w)^n, \tag{25}$$

where $\Gamma(\cdot)$ is the Gamma function and $\psi(\cdot)$ the Psi (Digamma) function. In general, Eq. (25) exhibits satisfactory rate of convergence even when evaluating the limit of the hypergeometric function as $w \to 1^-$. Finally, for $w \in (-\infty, -1/2)$, the following linear transformation is used [14]:

$$ {}_2F_1(a,b,c;w) = (1-w)^{-a} \, {}_2F_1\left(a, c-b, c; \frac{w}{w-1}\right). \tag{26}$$

The new function evaluation falls into one of the cases covered by Eqs. (24) and (25).

References

[1] R. Bouc, Forced vibration of mechanical systems with hysteresis, *Proceedings of the Fourth Conference on Non-linear oscillation*, Prague, Czechoslovakia, 1967.
[2] Y.K. Wen, Method for random vibration of hysteretic systems, *Journal of the Engineering Mechanics Division* 102 (2) (1976) 249–263.
[3] M.V. Sivaselvan, A.M. Reinhorn, Hysteretic models for deteriorating inelastic structures, *ASCE Journal of Engineering Mechanics* 126 (6) (2000) 633–640.
[4] C.-H. Wang, S.-Y. Chang, Development and validation of a generalized biaxial hysteresis model, *ASCE Journal of Engineering Mechanics* 133 (2) (2007) 141–152.
[5] Y.Q. Ni, J.M. Ko, C.W. Wong, Identification of non-linear hysteretic isolators from periodic vibration tests, *Journal of Sound and Vibration* 217 (4) (1998) 737–756.
[6] G.C. Foliente, Hysteresis modeling of wood joints and structural systems, *ASCE, Journal of Structural Engineering* 121 (6) (1995) 1013–1022.
[7] N.M. Kwok, Q.P. Ha, M.T. Nguyen, J. Li, B. Samali, Bouc–Wen model parameter identification for a MR fluid damper using computationally efficient GA, *ISA Transactions* 46 (2007) 167–179.
[8] F. Xia, Modelling of a two-dimensional Coulomb friction oscillator, *Journal of Sound and Vibration* 256 (2003) 1063–1074.
[9] F. Ma, H. Zhang, A. Bockstedte, G.C. Foliente, P. Paevere, Parameter analysis of the differential model of hysteresis, *Journal of Applied Mechanics ASME* 71 (2004) 342–349.
[10] M.C. Constantinou, M.A. Adnane, Dynamics of soil-base-isolated structure systems: evaluation of two models for yielding systems, Report to NSAF, Department of Civil Engineering, Drexel University, Philadelphia, PA, 1987.

[11] M.V. Sivaselvan, A.M. Reinhorn, Hysteretic models for deteriorating inelastic structures, *ASCE Journal of Engineering Mechanics* 126 (6) (2000) 633–640.
[12] S. Erlicher, N. Point, Thermodynamic admissibility of Bouc–Wen type hysteresis models, *Comptes Rendus Mécanique* 332 (2004) 51–57.
[13] W.H. Press, S.A. Teukolsky, W.T. Vetterling, B.P. Flannery, *Numerical Recipes in C++: The Art of Scientific Computing*, Cambridge University Press, Cambridge, 2002.
[14] M. Abramowitz, I.A. Stegun, Handbook of Mathematical Functions, National Bureau of Standards, Washington (reprinted 1972 by Dover Publications, New York).
[15] F. Ikhouane, J. Rodellar, On the hysteretic Bouc–Wen model, part I: forced limit cycle characterization, *Nonlinear Dynamics* 42 (2005) 63–78.
[16] F. Naiem, J.M. Kelly, *Design of Seismic Isolated Structures*, Wiley, New York, 1999.